Preparation of Size-Selective Nanoporous Polymer Networks of Aromatic Rings: Potential Adsorbents for Hydrogen Storage

Jonathan Germain,[†] Frantisek Svec,*[,‡] and Jean M. J. Fréchet*[,†,‡]

College of Chemistry, University of California, Berkeley, California 94720-1460, and The Molecular Foundry, Lawrence Berkeley National Laboratory, Berkeley, California 94720-8139

Received August 7, 2008. Revised Manuscript Received September 22, 2008

The preparation of nanoporous size-selective hypercrosslinked polymer networks containing 37−92% of pores small enough for hydrogen adsorption but too small to allow penetration of nitrogen has been studied. Polyaniline and diaminobenzene were coupled with diiodobenzene and tribromobenzene using Ullman and Buchwald synthetic routes. The resulting porous polymer networks consist of aromatic rings linked through a trivalent nitrogen atom. The Buchwald reaction appears to be more effective than the Ullman synthesis for the production of such materials. The use of solvents with higher Hildebrand solubility coefficients during synthesis affords polymers with higher surface areas. The nanoporous polymers possess unusually high initial enthalpies of adsorption of hydrogen reaching values of up to −18 kJ/mol.

Introduction

Nanoporous polymers fall into three broad categories. (i) Crosslinked polymers prepared via polymerization in the presence of a porogen, which have surface areas of up to about 1000 m^2/g and have been used extensively as separation media for several decades.[1,2] (ii) Hypercrosslinked polymers, with achievable surface areas of more than 2000 m^2/g.[3−12] (iii) Polymers with intrinsic microporosity with surface areas reaching 1000 m^2/g.[13,14] Nanoporous polymers are drawing significant attention because of a variety of emerging applications in electrodes[15] chromatography[16−19] and in hydrogen storage,[7,8,13,14,20−25] where these materials may play a pivotal role.

Hydrogen is one of the alternative fuels envisioned to decrease both carbon dioxide emissions and dependency on oil related products. However, the development of a hydrogen economy requires the development of safe, lightweight, and high capacity storage systems for hydrogen. The U.S. Department of Energy has set a target that requires the development of systems able to store 6 wt % hydrogen by the year 2010.[26] Nanoporous polymers have recently been found as promising adsorbents for hydrogen storage that show a potential to help meet this target. [7,8,13,14,20−25]

Although the surface area and pore volume of any nanoporous material determine its capacity, the enthalpy of adsorption ΔH determines the temperatures at which hydrogen is adsorbed and released. A wealth of high surface area materials including metal-organic frameworks (MOF),[27−35] porous polymers, [7,8,13,14,20−25] and porous carbons[36] have been synthesized that offer high hydrogen storage capacities at cryogenic temperatures. Unfortunately, attempts to extend their hydrogen storage capabilities to room temperature have

* To whom correspondence should be addressed. Fax: (510) 643-3077. E-mail: fsvec@lbl.gov (F.S.); frechet@berkeley.edu (J.M.J.F.).
[†] University of California, Berkeley.
[‡] Lawrence Berkeley National Laboratory.

(1) Guyot, A.; Bartholin, M. *Prog. Polym. Sci.* **1982**, *8*, 277.
(2) Okay, O. *Prog. Polym. Sci.* **2000**, *25*, 711.
(3) Davankov, V. A.; Tsyurupa, M. P. *React. Polym.* **1990**, *13*, 27.
(4) Pastukhov, A. V.; Tsyurupa, M. P.; Davankov, V. A. *J. Polym. Sci., Polym. Phys.* **1999**, *37*, 2324.
(5) Ahn, J.; Jang, J.; Oh, C.; Ihm, S.; Cortez, J.; Sherrington, D. C. *Macromolecules* **2005**, *39*, 627.
(6) Tsyurupa, M. P.; Davankov, V. A. *React. Funct. Polym.* **2006**, *66*, 768.
(7) Germain, J.; Hradil, J.; Fréchet, J. M. J.; Svec, F. *Chem. Mater.* **2006**, *18*, 4430.
(8) Wood, C. D.; Tan, B.; Trewin, A.; Niu, H.; Bradshaw, D.; Rosseinsky, M. J.; Khimyak, Y. Z.; Campbell, N. L.; Kirk, R.; Stockel, E.; Cooper, A. I. *Chem. Mater.* **2007**, *19*, 2034.
(9) Dawson, R.; Su, F. B.; Niu, H. J.; Wood, C. D.; Jones, J. T. A.; Khimyak, Y. Z.; Cooper, A. I. *Macromolecules* **2008**, *41*, 1591.
(10) Jiang, J. X.; Su, F.; Trewin, A.; Wood, C. D.; Campbell, N. L.; Niu, H.; Dickinson, C.; Ganin, A. Y.; Rosseinsky, M. J.; Khimyak, Y. Z.; Cooper, A. I. *Angew. Chem., Int. Ed.* **2007**, *46*, 8574.
(11) Jiang, J. X.; Su, F.; Niu, H.; Wood, C. D.; Campbell, N. L.; Khimyak, Y. Z.; Cooper, A. I. *Chem. Commun.* **2008**, 486.
(12) Jiang, J. X.; Su, F.; Trewin, A.; Wood, C. D.; Niu, H.; Jones, J. T. A.; Khimyak, Y. Z.; Cooper, A. I. *J. Am. Chem. Soc.* **2008**, *130*, 7710.
(13) McKeown, N. B.; Gahnem, B.; Msayib, K. J.; Budd, P. M.; Tattershall, C. E.; Mahmood, K.; Tan, S.; Book, D.; Langmi, H. W.; Walton, A. *Angew. Chem., Int. Ed.* **2006**, *45*, 1804.
(14) Ghanem, B. S.; Msayib, K. J.; McKeown, N. B.; Harris, K. D. M.; Pan, Z.; Budd, P. M.; Butler, A.; Selbie, J.; Book, D.; Walton, A. *Chem. Commun.* **2007**, 67.
(15) Chen, W. C.; Wen, T. C.; Teng, H. S. *Electrochim. Acta* **2003**, *48*, 641.
(16) Svec, F.; Kurganov, A. A. *J. Chromatogr., A* **2008**, *1184*, 281.
(17) Svec, F. *J. Sep. Sci.* **2004**, *27*, 1419.
(18) Rohr, T.; Hilder, E. F.; Donovan, J. J.; Svec, F.; Fréchet, J. M. J. *Macromolecules* **2003**, *36*, 1677.
(19) Sykora, D.; Peters, E. C.; Svec, F.; Fréchet, J. M. J. *Macromol. Mater. Eng.* **2000**, *275*, 42.
(20) Lee, J. Y.; Wood, C. D.; Bradshaw, D.; Rosseinsky, M. J.; Cooper, A. I. *Chem. Comm.* **2006**, 2670.
(21) Germain, J.; Svec, F.; Fréchet, J. M. J. *PMSE Prepr. (ACS, Div. Polym. Chem.)* **2007**, *97*, 272–273.
(22) Germain, J.; Fréchet, J. M. J.; Svec, F. *J. Mater. Chem.* **2007**, *17*, 4989.
(23) McKeown, N. B.; Budd, P. M. *Chem. Soc. Rev.* **2006**, *35*, 675.
(24) McKeown, N. B.; Budd, P. M.; Book, D. *Macromol. Rapid Commun.* **2007**, *28*, 995.
(25) Budd, P. M.; Butler, A.; Selbie, J.; Mahmood, K.; McKeown, N. B.; Ghanem, B.; Msayib, K.; Book, D.; Walton, A. *Phys. Chem. Chem. Phys.* **2007**, *9*, 1802.
(26) Schlapbach, L.; Zuttel, A. *Nature* **2001**, *414*, 353.

10.1021/cm802157r CCC: $40.75
Published on Web 10/29/2008

been hampered by their small hydrogen adsorption enthalpies. Theoretical calculations indicate that an enthalpy of adsorption in the range of 15−20 kJ/mol is needed to achieve hydrogen adsorption at room temperature,[37] but most of the materials examined thus far exhibit ΔH values that do not exceed 4−7 kJ/mol. One option to increase this key metric is to develop materials with new chemistries. Thus, Dinca et al. have designed MOFs that exhibit enthalpies of adsorption between −9.5 and −10.5 kJ/mol, which they suggest is due to the presence of exposed magnesium,[31] copper,[35] and manganese[34] centers. However, Paella et al. have later suggested different interpretations of the mechanism that enables such high adsorption enthalpies.[38] We have prepared nanoporous hypercrosslinked polyanilines featuring $\Delta H = -9.3$ kJ/mol. Another approach to an increase in ΔH is the preparation of adsorbents with a very small pore size. This strategy has been both predicted by theory[39] and demonstrated by experiment.[40] An increase in adsorption enthalpy is thought to occur as a result of higher solid−fluid interaction potentials due to simultaneous interaction of the fluid with multiple pore walls.[41]

Analysis of this concept leads to the conclusion that the highest achievable enthalpy of adsorption must be exhibited by materials with pore sizes similar to the kinetic diameter of the hydrogen molecule. Pores that are larger should have lower adsorption enthalpies while smaller pores are inaccessible. In this work, we describe our approach to nanoporous polymeric networks with well-controlled pore size formed by linking aromatic rings. These polymers contain a large number of pores that enable size discrimination between nitrogen and hydrogen molecules. While hydrogen can penetrate these pores, nitrogen is too bulky to enter them. Unlike porous materials that are typically used in membranes,[42−44] the selectivity of our polymers is based on thermodynamic rather than kinetic attributes. Our novel insoluble rigid polymers display ΔH values as high as −18 kJ/mol for hydrogen adsorption.

Experimental Section

Materials and Equipment. Polyaniline, diiodobenzene, tribromobenzene, diaminobenzene, dibromobenzene and anhydrous *N*-methyl pyrrolidinone were purchased from Aldrich (St. Louis, MO). Dimethylformamide and toulene were purified using a solvent purification system before use.[45] All other solvents were of the best available quality and used without additional purification.

Hydrogen (99.999% purity) and nitrogen (99.9995% purity) adsorption measurements at pressures of up to 0.12 MPa were carried out on a Micromeritics ASAP 2020 (Norcross, GA) surface area and porosity analyzer as described elswhere.[7] The porous polymers were degassed at 110−115 °C. High-pressure hydrogen adsorption measurements were carried out with a PCT Pro 2000 (Hy-Energy, Newark, CA). Samples were first degassed on the ASAP 2020 instrument, then moved to a nitrogen filled glovebox where they were transferred into the PCT Pro 2000 sample holder. To remove nitrogen from the system, the sample holder was flushed with helium several times before measurements began. Because the PCT Pro does not have a turbopump, an adapter was used to degas PCT Pro samples using the ASAP 2020. The Brunauer−Emmett−Teller (BET) equation was used to calculate specific surface areas based on nitrogen adsorption isotherms measured at 77 K and relative pressures approaching 1.0. The Langmuir equation was used to calculate specific surface areas based on hydrogen adsorption isotherms measured at 77 K and pressures of up to 0.12 MPa. Enthalpy of adsorption was calculated by applying the van't Hoff equation to pairs of adsorption isotherms measured at 273 and 295 K.

Microwave-assisted reactions were carried out a Biotage Initiator 2.0 (Biotage, Inc., Uppsala, Sweden).

Elemental analyses were conducted by Quantitative Technologies, Inc. (Whitehouse, NJ). Infrared spectra were collected using an Excalibur 3100 FT-IR (Varian, Inc., Palo Alto, CA). Dry polymers were mixed with KBr and formed into pellets within a nitrogen filled glovebox. The resulting KBr pellets were transported to the IR and characterized as quickly as possible.

Preparation of Bromotris(triphenylphosphine) Copper(I). A soluble copper catalyst was synthesized acording to Gujadhur et al.[46] Triphenylphosphine (30.7 g) of was added to 500 mL of boiling methanol and allowed to dissolve. Copper(II) bromide (6.2 g) was added and the mixture refluxed for 10 min while a white precipitate was formed. The mixture was cooled to room temperature, the liquid filtered off, and the solid rinsed on a Buchner funnel with ethanol and diethyl ether. The recovered solid was then dried at room temperature in vacuo.

Preparation of Leucoemeraldine Polyaniline. Leucoemeraldine polyaniline was prepared using a modified method of Moon et al.[47] In a typical synthesis, 200 mL of water was purged with nitrogen and added to 20 g of emeraldine base polyaniline and 40 g of sodium dithionite. Another 20 g portion of dithionite was added after 6 h. The dispersion was allowed to stir overnight, and the solid then decanted in 1.5 L of water that had first been purged with nitrogen to lower its oxygen content. After separation, the solid polymer was dried in vacuo at room temperature and stored in a desiccator under vacuum. The reduction to leucoemeraldine polyaniline was verified by the disappearance of the peak at about 630 nm in the UV−vis spectrum.[47]

(27) Wong-Foy, A. G.; Matzger, A. J.; Yaghi, O. M. *J. Am. Chem. Soc.* **2006**, *128*, 3494.
(28) Rowsell, J. L. C.; Eckert, J.; Yaghi, O. M. *J. Am. Chem. Soc.* **2005**, *127*, 14904.
(29) Furukawa, H.; Miller, M. A.; Yaghi, O. M. *J. Mater. Chem.* **2007**, *17*, 3197.
(30) Kaye, S. S.; Dailly, A.; Yaghi, O. M.; Long, J. R. *J. Am. Chem. Soc.* **2007**, *129*, 14176.
(31) Dinca, M.; Long, J. R. *J. Am. Chem. Soc.* **2005**, *127*, 9376.
(32) Kaye, S. S.; Long, J. R. *J. Am. Chem. Soc.* **2005**, *127*, 6506.
(33) Dinca, M.; Dailly, A.; Liu, Y.; Brown, C. M.; Neumann, D. A.; Long, J. R. *J. Am. Chem. Soc.* **2006**, *128*, 16876.
(34) Dinca, M.; Long, J. R. *J. Am. Chem. Soc.* **2007**, *129*, 11172.
(35) Dinca, M.; Han, W. S.; Liu, Y.; Dailly, A.; Brown, C. M.; Long, J. R. *Angew. Chem., Int. Ed.* **2007**, *46*, 1419.
(36) Pacula, A.; Mokaya, R. *J. Phys. Chem.C* **2008**, *112*, 2764.
(37) Bhatia, S. K. *Langmuir* **2006**, *22*, 1688.
(38) Panella, B.; Hones, K.; Muller, U.; Trukhan, N.; Schubert, M.; Putter, H.; Hirscher, M. *Angew. Chem., Int. Ed.* **2008**, *47*, 2138.
(39) Kowalczyk, P.; Tanaka, H.; Holyst, R.; Kaneko, K.; Ohmori, T.; Miyamoto, J. *J. Phys. Chem. B* **2005**, *109*, 17174.
(40) Jhung, S. H.; Kim, H. K.; Yoon, J. W.; Chang, J. S. *J. Phys. Chem. B* **2006**, *110*, 9371.
(41) Wang, Q. Y.; Johnson, J. K. *J. Chem. Phys.* **1999**, *110*, 577.
(42) Freeman, B. D. *Macromolecules* **1999**, *32*, 375.
(43) Stern, S. A. *J. Membr. Sci.* **1994**, *94*, 1.
(44) Illing, G.; Hellgardt, K.; Wakeman, R. J.; Jungbauer, A. *J. Membr. Sci.* **2001**, *184*, 69.
(45) Pangborn, A. B.; Giardello, M. A.; Grubbs, R. H.; Rosen, R. K.; Timmers, F. J. *Organometallics* **1996**, *15*, 1518.
(46) Gujadhur, R.; Venkataraman, D.; Kintigh, J. T. *Tetrahedron Lett.* **2001**, *42*, 4791.
(47) Moon, D. K.; Ezuka, M.; Maruyama, T.; Osakada, K.; Yamamoto, T. *Makromol. Chem.* **1993**, *194*, 3149.

Hypercrosslinking of Leucoemeraldine Polyaniline with 1,4-Dibromobenzene Using Copper(II) Bromide (Entry 1). Leucoemeraldine polyaniline was crosslinked using a synthesis based on the method of Ito, et al.[48] A dry microwave vial was charged with 0.30 g of leucoemeraldine polyaniline, 2.07 g of potassium carbonate and 1.59 g of p-dibromobenzene and mixed. The vial was flushed with dry nitrogen followed by addition of 4 mL of anhydrous DMF added. The vial was shaken to allow the solids to dissolve and 0.48 g of copper(II) bromide added. The vial was sealed and placed in the microwave reactor at 200 °C for 2 h.

Hypercrosslinking Using Buchwald Syntheses.[49] *Leucoemeraldine Polyaniline with 1,4-Diiodobenzene (Entries 5−7).* In a typical synthesis, 0.23 g of leucoemeraldine polyaniline, 0.17 g of 1,1′-bis(diphenylphosphino)-ferrocene, 0.51 g of 1,4-diiodobenzene, 1.0 g of sodium t-butoxide, and 0.17 g of bis(dibenzy-lideneacetone) dipalladium(0) were loaded into a microwave vial inside a nitrogen-filled glovebox. The microwave vial was sealed and 3 mL of anhydrous DMF added. The system was allowed to react in the microwave reactor at 170 °C for 2 h.

1,4-Diaminobenzene with 1,4-Diiodobenzene (Entry 8). 1.2 g 1,4-diaminobenzene, 4.7 g of sodium t-butoxide, 8.1 g of p-diiodobenzene, 0.7 g of 1,1′-bis(diphenylphosphino)ferrocene, and 0.7 g of bis(dibenzylideneacetone) dipalladium(0) were loaded into a microwave vial inside a nitrogen-filled glovebox. The microwave vial was sealed, 12 mL of anhydrous DMF added, and the reaction carried out in the microwave reactor at 200 °C for 2 h.

1,4-Diaminobenzene with 1,3,5-Tribromobenzene (Entry 9). One and one-tenth of a gram of p-diaminobenzene, 4.7 g of sodium t-butoxide, 3.2 g of 1,3,5 tribromobenzene, 0.7 g of 1,1′-bis(diphenylphosphino)ferrocene, and 0.7 g of bis(dibenzylideneacetone) dipalladium(0) were loaded into a microwave vial inside a nitrogen-filled glovebox. The microwave vial was sealed, 12 mL of anhydrous DMF was added, and the reaction was carried out in the microwave reactor at 200 °C for 2 h.

Leucoemeraldine Polyaniline (5000 MW) with 1,3,5-Tribromobenzene (Entry 10). Leucoemeraldine polyaniline (1.583 g), 1.82 g of sodium t-butoxide, 1.82 g of 1,3,5-tribromobenzene, 0.6 g of 1,1′-bis(diphenylphosphino)ferrocene, and 0.6 g of bis(dibenzylideneacetone) dipalladium(0) were loaded into a microwave vial inside a nitrogen-filled glovebox. The microwave vial was sealed and 10 mL of anhydrous DMF was added. The system was allowed to react in the microwave reactor for 2 h at 170 °C.

Leucoemeraldne Polyaniline (100 000 MW) with 1,3,5-Tribromobenzene (Entry 11). Ninety-three hundredths of a gram of leucoemeraldine polyaniline, 1.07 g of sodium t-butoxide, 1.04 g of 1,3,5-tribromobenzene, 0.7 g of 1,1′-bis(diphenylphosphino)ferrocene, and 0.7 g of bis(dibenzylideneacetone) dipalladium(0) were loaded into a microwave vial inside a nitrogen-filled glovebox. The microwave vial was sealed and 10 mL of anhydrous DMF added. The system was allowed to react in the microwave reactor at 200 °C for 2 h.

Leucoemeraldine Polyaniline (5000 MW) with 1,3,5-Tribromobenzene (Entry 12). Polyaniline was cross-linked with *p*-diiodobenzene using a Buchwald synthesis.[49] Ninety-three hundredths of a gram of leucoemeraldine polyaniline, 1.09 g of sodium t-butoxide, 1.04 g of 1,3,5-tribromobenzene, 0.7 g of 1,1′-bis(diphenylphosphino)ferrocene, and 0.7 g of bis(dibenzylideneacetone) dipalladium(0) were loaded into a microwave vial inside a nitrogen-filled glovebox. The microwave vial was sealed and 10 mL of anhydrous DMF were added. The system was allowed to react in the microwave reactor for 2 h at 200 °C.

Hypercrosslinking Using Ullman Syntheses, Based on the Method of Gujadhur, et al.[46] *Leucoemeraldine Plyaniline (5000 MW) with* p-*Diiodobenzene Using Bromotris(Triphenylphosphine) Copper(I) (Entries 2−4).* In a typical synthesis, 0.23 g of leucoemeraldine polyaniline, 3.0 g of cesium carbonate, and 1.5 g of $Cu(PPh_3)_3Br$ catalyst were mixed in a microwave vial. The vial was flushed with dry nitrogen and 3 mL of the anhydrous solvent was added. The vial was then sealed and placed in the microwave reactor at 200 °C for 1 h.

1,4-Diaminobenzene with 1,3,5-Tibromobenzene (Entry 13). Seventy-eight hundreths of a gram of 1,4-diaminobenzene, 14 g of cesium carbonate, 3.0 g of 1,3,5-tribromobenzene, and 1.6 g of bromo(triphenylphosphine) copper(I) were loaded into a microwave vial inside a nitrogen-filled glovebox. The microwave vial was sealed, 9 mL of anhydrous DMF was added, and the reaction was carried out in the microwave reactor at 195 °C for 12 h.

Recovery and Purification of Hypercrosslinked Polymers. Following each hypercrosslinking reaction, the polymer was recovered and extracted with DMF in a Soxhlet apparatus until the solvent around the thimble was visually clear for at least one day. The polymers were recovered by filtration and then placed in a solution of NaOH in methanol for a few minutes. Finally, the solid was rinsed with water until the effluent had a neutral pH. To speed drying, the polymers were then rinsed with diethyl ether before being dried in vacuo at room temperature.

Thermal Purification of Hypercrosslinked Polymers. The polymers were evacuated on an ASAP 2010 or 2020 at room temperature until the pressure in the vial was less than 0.005 torr. The polymers were then heated to 450 °C while remaining under a vacuum. In cases where residue appeared on the side of a vial, the polymers were moved to new vials. Heat treatment was considered complete when the pressure in a vial was reduced to 1×10^{-6} torr.

Results and Discussion

Preparation of Nanoporous Polymers. In this study, we targeted networks consisting of aromatic rings held in a porous framework by the smallest possible linking groups. The reasons for this approach are two-fold. First, we have shown previously that nanoporous polymers prepared via hypercrosslinking using smaller, more rigid cross-links exhibit higher surface areas than those synthesized with longer, less-rigid cross-links.[22] Second, smaller cross-links add less nonadsorbing mass to the final porous material. We also wanted to avoid the presence of electron withdrawing substituents on the aromatic rings because we have already demonstrated that addition of electron withdrawing groups to aromatic rings decreases their ability to physisorb hydrogen.[21,22]

The simplest approach to forming networks consisting of aromatic rings starts with precursors containing reactive groups directly attached to the aromatic ring such as aryl halides and amines, which can be coupled using a variety of synthetic routes. For example, the Ullman reaction catalyzed with soluble[46] or insoluble[48] copper salts and the Buchwald reaction [49−51] which relies on soluble palladium catalysts are used often to perform such couplings. As shown in Scheme 1, both of these syntheses were applied to the crosslinking of aryl amines with polyhalogenobenzenes to

(48) Ito, A.; Ino, H.; Tanaka, K.; Kanemoto, K.; Kato, T. *J. Org. Chem.* **2002**, *67*, 491.
(49) Yang, B. H.; Buchwald, S. L. *J. Organomet. Chem.* **1999**, *576*, 125.
(50) Agou, T.; Kobayashi, J.; Kawashima, T. *Org. Lett.* **2006**, *8*, 2241.
(51) Wolfe, J. P.; Tomori, H.; Sadighi, J. P.; Yin, J. J.; Buchwald, S. L. *J. Org. Chem.* **2000**, *65*, 1158.

Scheme 1. Components and Reactions Used to Prepare Nitrogen-Linked Nanoporous Networks of Aromatic Rings, And Representative Structures thereof: (A) Ullman Reaction Catalyzed by Insoluble CuBr, [46] (B) Ullman Reaction Catalyzed by Soluble $Cu(PPh_3)_3Br$, [48] (C) Buchwald Reaction Catalyzed by Soluble $Pd(dba)_2$[49−51]

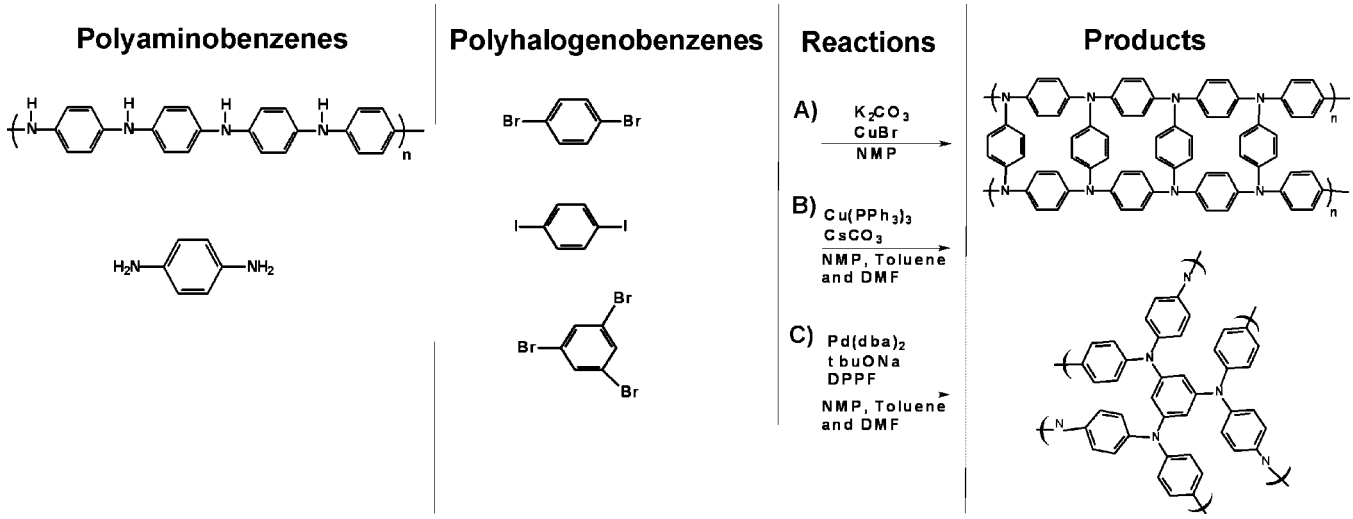

Table 1. Porous Properties of Polymeric Networks of Aromatic Rings Synthesized from Leucoemeraldine and Dihalobenzenes

			surface area (m^2/g)				
entry	synthesis	solvent	BET[a]	Langmuir[b]	$V_{p,tot}$[c] (cm^3/g)	$V_{p,nano}$[d] (cm^3/g)	H_2[e] (wt %)
1	Ullman/insoluble	DMF	54	156	0.13	0.03	0.38
2	Ullman/soluble	NMP	1	0	0.01	0.00	0.01
3	Ullman/soluble	toluene	13	27	0.07	0.01	0.06
4	Ullman/soluble	DMF	18	96	0.04	0.01	0.19
5	Buchwald	NMP	17	66	0.01	0.00	0.13
6	Buchwald	toluene	5	41	0.02	0.00	0.11
7	Buchwald	DMF	113	135	0.46	0.05	0.30
7[f]	Buchwald	DMF	316	343	0.25	0.13	0.85

[a] Calculated from nitrogen adsorption isotherms using the BET equation. [b] Calculated from hydrogen adsorption isotherms using the Langmuir equation. [c] Total pore volume calculated from nitrogen adsorption at a relative pressure of 0.99. [d] Nanopore volume estimated from nitrogen adsorption at a relative pressure of 0.25. [e] Hydrogen storage capacity at 77 K and 0.12 MPa. [f] After thermal purification at 450 °C in a vacuum.

form amine-linked networks of aromatic rings. Thus crosslinking with tribromobenzene affords networks of di- and trifunctionalized aromatic rings connected by amines whereas crosslinking with diiodoobenzene or dibromobenzene leads to a network of difunctionalized aromatic rings. Although the substituted benzenes can be considered cross-linkers from the synthetic point of view, the final product is in fact a network of aromatic rings connected through nitrogen atoms. As is typically the case with hypercrosslinked polymers, complete conversion of all functional groups is not achievable. Although the IR spectra of our materials lack the sharp N−H stretching peak near 3348 cm^{-1}, which is characteristic of secondary amines in leucoemeraldine base polyaniline,[52,53] it is possible that a small amount of secondary amine is also present alongside the tertiary amines. Therefore, Scheme 1 shows only the expected structure, not including any impurity that may result from incomplete functionalization. Because of the rapid and random nature of the reaction systems used for their preparation, all of the products are amorphous, crosslinked networks.

Regardless of whether soluble or insoluble copper catalysts were used, Ullman syntheses lead to polymers that contain both copper and iodine. In contrast, the Buchwald reaction affords materials with no remaining iodine. The presence of copper in the final product adds unnecessary mass to our materials, whereas the presence of iodine both adds mass and demonstrates that Ullman cross-linking is incomplete. Because the Buchwald approach results in halogen-free materials with higher surface areas, it was selected as the synthetic method of choice for the remainder of this study.

In hypercrosslinking, a precursor is either swollen or dissolved in a solvent, then cross-linked to form a network before the partially cross-linked polymer can desolvate. Thus, hypercrosslinking is a process that relies on the kinetics of two competitive reactions: the crosslinking reaction, and the desolvation of the polymer being crosslinked.[22] As a result, the choice of solvent has a profound impact on the ultimate surface areas achieved for the hypercrosslinked polyanilines. Initial expectations were that solvents with Hildebrand solubility parameters[54] close to that of polyaniline would produce materials with the highest surface areas. However, we found that materials with higher surface areas were obtained from reactions carried out in solvents with the highest Hildebrand solubility parameters (Table 1). Toluene, which has a Hildebrand solubility parameter of 18.2 $MPa^{1/2}$,[54] affords nanoporous polymers with lower surface areas than those prepared in N-methyl pyrrolidinone (23.1 $MPa^{1/2}$) or dimethylformamide (24.8 $MPa^{1/2}$).

(52) Zheng, W. Y.; Levon, K.; Laakso, J. *Macromolecules* **1994**, *27*, 7754.
(53) Ping, Z.; Nauer, G. E.; Neugebauer, H.; Theiner, J. *J. Electroanal. Chem.* **1997**, *420*, 301.
(54) Brandrup, J.; Immergut, E. H.; Grulke, E. A.; Abe, A.; Bloch, D. R.; Eds. *Polymer Handbook*, 4th ed.; Wiley: New York, 2005.

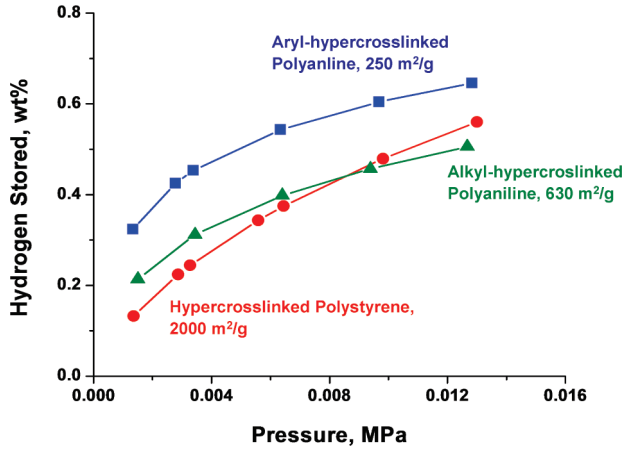

Figure 1. Low pressure hydrogen adsorption by hypercrosslinked polystyrene with a surface area of 2000 m^2/g as calculated by application of the BET equation to N_2 adsorption isotherms (circles), alkyl-hypercrosslinked polyanilines with 630 m^2/g (triangles), and a polymer network of aromatic rings (**9**) with 250 m^2/g (squares).

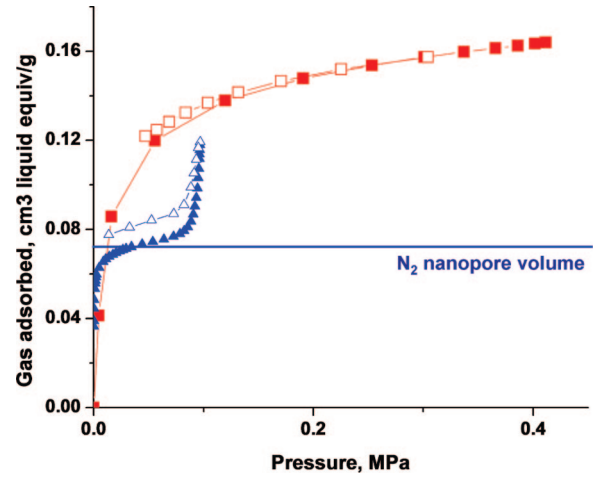

Figure 2. Adsorption capacity of nanopores available to hydrogen (squares) and nitrogen (triangles) in polymer **11**. Adsorption is marked with filled shapes, desorption is marked with empty shapes. The size-selective pore volume can be determined from difference between the volumes available to N_2 and H_2.

FTIR spectra of the polymeric networks of aromatic rings hypercrosslinked using the Buchwald process show the presence of residual phosphorus oxidation products even after extensive Soxhlet extraction with DMF. To remove these impurities, the polymers were heated at 450 °C under a vacuum to remove small molecules from the polymer. The release of material was observed visually as some material accumulated on the sides of the heated sample tube. In addition, the IR bands at ~1110 cm^{-1}, which is associated with products of the oxidation of phenyl phosphorus compounds[55] and the band at ~1300 cm^{-1}, which appears in the spectrum of 1,1′-bis(diphenylphosphino)-ferrocene (DPPF) either disappeared entirely or diminished substantially. Comparison with the FTIR spectrum of DPPF suggests that several of the peaks between 1900 and 1770 cm^{-1}, which either disappear or are greatly reduced during thermal purification, originate from residual catalyst. Just as importantly, the specific surface areas of materials such as polymer **7** more than doubled as a result of this treatment.

Gas Sorption Characteristics. Low pressure hydrogen adsorption isotherms shown in Figure 1 demonstrate an interesting result. Our network of aromatic rings with a BET surface area of about 250 m^2/g adsorb more hydrogen at low pressures than hypercrosslinked polystyrenes with surface areas more than seven times as large. In addition, these materials exhibit Langmuir surface areas calculated using H_2 adsorption isotherms larger than those calculated using the BET equation and nitrogen adsorption isotherms. Typically, larger BET surface areas compared to Langmuir are observed due to capillary condensation[56] as has been previously documented for porous polymers.[8,22,25] This unexpected observation and the high hydrogen adsorption at low pressures suggest high H_2-polymer interaction energies in our networks of aromatic rings.

Nitrogen adsorption isotherms are commonly used to determine the pore volume available for adsorption of N_2 molecules. Because the density of supercritical hydrogen must be smaller than that of liquid hydrogen, we use hydrogen adsorption isotherms to perform similar calculations and find the pore volume accessible to H_2.[57] Upon completion of these calculations, it becomes obvious that a substantial portion of the pore volume in these nanoporous polymers includes pores that are large enough for accommodate hydrogen while excluding nitrogen. As shown in Figure 2 and Table 2, the actual hydrogen storage capacity for most of the networks of aromatic rings in this study exceeds the capacity that could be realized in nitrogen-accessible nanopores. Several authors have estimated the diameters of adsorbed H_2[58,59] and N_2;[60] we believe that these pores are between 0.29 and 0.36 nm in size. Earlier work on polyaniline hypercrosslinked with methylene groups reported the formation of pores that were 1−2 nm in diameter and therefore large enough for adsorption of nitrogen.[22] Pores of the small size observed in our polymers are formed when aromatic rings are connected by a trivalent, rigid linker, the nitrogen atom in this case.

It is well understood that only pores smaller than about 3 nm play a substantial role in hydrogen adsorption.[61,62] These pores can be divided into three categories: (i) pores in which two hydrogen molecules cannot pass each other and only single-file diffusion can occur,[63,64] (ii) pores with entranceways too small for nitrogen to pass but large enough for hydrogen, and (iii) pores in which both hydrogen and nitrogen can be accommodated. In the third type of pores, adsorption is fast, as typical diffusion prevails and adsorption enthalpies decrease with increasing surface coverage. Single-

(55) Ma, K.; vandeVoort, F. R.; Sedman, J.; Ismail, A. A. *J. Am. Oil Chem. Soc.* **1997**, *74*, 897.
(56) Kaneko, K.; Ishii, C. *Colloids Surf.* **1992**, *67*, 203.
(57) Zuttel, A.; Sudan, P.; Mauron, P.; Wenger, P. *Appl. Phys. A: Mater. Sci. Process.* **2004**, *78*, 941.
(58) Negri, F.; Saendig, N. *Theor. Chem. Acc.* **2007**, *118*, 149.
(59) Schimmel, H. G.; Kearley, G. J.; Nijkamp, M. G.; Visserl, C. T.; de Jong, K. P. *Chem.—Eur. J.* **2003**, *9*, 4764.
(60) Lushington, G. H.; Chabalowski, C. F. *Theochem. J. Mol. Struct* **2001**, *544*, 221.
(61) Dillon, A. C.; Heben, M. J. *Appl. Phys. A: Mater. Sci. Process.* **2001**, *72*, 133.
(62) Thomas, K. M. *Catal. Today* **2007**, *120*, 389.
(63) Sholl, D. S.; Fichthorn, K. A. *J. Chem. Phys.* **1997**, *107*, 4384.
(64) Wei, Q. H.; Bechinger, C. *Science* **2000**, *287*, 625.

Table 2. Porous Properties of Polyaniline and Diaminobenzene Hypercrosslinked in Dimethylformamide Using Buchwald Conditions, After Thermal Purification

		surface area (m^2/g)					
entry	amine/halobenzene	BET[a]	Langmuir[b]	H_2[c](wt %)	$V_{p,tot}$[d](cm^3/g)	$V_{P,\ nano}$[e](cm^3/g)	$V_{P,\ ultra}$[f] (cm^3/g)
8	diaminobenzene/diiodobenzene	17	192	0.47	0.01	0.01	0.09
9	diaminobenzene/tribromobenzene	249	384	0.97	0.13	0.11	0.06
10	5000 MW leucoemeraldine polyaniline/tribromobenzene	5	186	0.47	0	0	0.14
11	100 000 MW leucoemeraldine polyaniline/tribromobenzene	157	354	0.89	0.11	0.06	0.11
12	5000 MW leucoemeraldine polyaniline/tribromobenzene	255	368	0.92	0.25	0.11	0.07

[a] Calculated from nitrogen adsorption isotherms using the BET equation. [b] Calculated from hydrogen adsorption using the Langmuir equation. [c] Hydrogen storage capacity at 77 K and 0.12 MPa. [d] Pore volume calculated from nitrogen adsorption at a relative pressure of 0.99. [e] Micropore volume estimated from nitrogen adsorption at a relative pressure of 0.25. [f] Volume of nanopores available to hydrogen but not nitrogen adsorption. All samples after heating to 450 °C in vacuum.

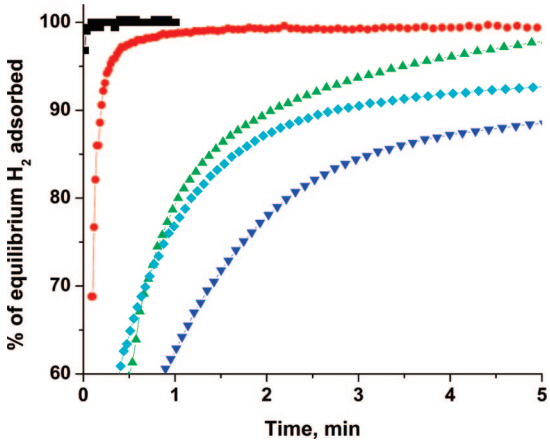

Figure 3. Kinetics of hydrogen adsorption to hypercrosslinked polystyrene[7] (squares), alkyl-hypercrosslinked polyaniline[22] (circles) and polymers **10** (triangles up), **13** (diamonds), and **8** (triangles down) at 77 K, upon dosing of the first aliquot of hydrogen.

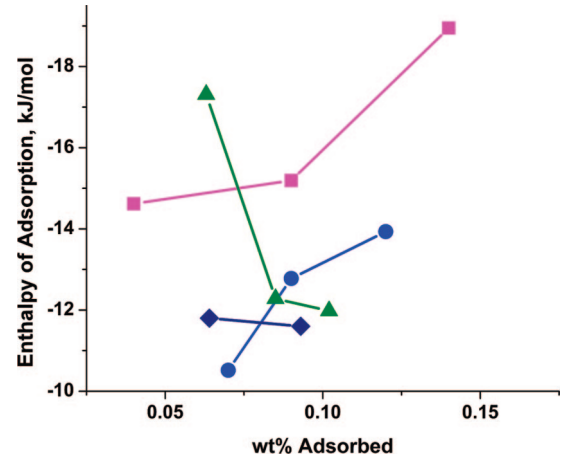

Figure 4. Enthalpy of hydrogen adsorption on polymers **8** (triangles), **9** (squares), **10** (circles), and **13** (diamonds) as calculated from isotherms measured at 273 and 295 K. The error margin is ±1 kJ/mol, as estimated from free space standard deviations used to determine instrument precision for each individual sample.

file diffusion occurs within a limited volume of the second type of pores but the majority of adsorption is achieved via ordinary Knudsen, Fickian, and surface diffusion. In contrast, the first type of pores allows only single-file diffusion. As shown in Table 2, the networks of aromatic rings we have prepared have large numbers of pores of the first and second type. Unfortunately, we have been unable to identify a method for determining the relative proportions of pores of the first and second type. Thermodynamic sieving by pore size has been observed in a few metal-organic frameworks[65−67] and coordination polymers.[68] Because most of these materials were crystalline, we can determine that N_2 was excluded by small apertures between pore volumes. This suggests that previous materials contained only pores of the second and third types.

As shown in Figure 3, adsorption in our size-selective pores is marked by drastically slower kinetics at cryogenic temperatures. Upon dosing the first aliquot of hydrogen at 77 K, both hypercrosslinked polystyrene and alkyl-hypercrosslinked polyanilines with pores in the range of 1−2 nm approach complete adsorption in less than one minute. All of the networks of aromatic rings with size-selective pores adsorb hydrogen more slowly. Polymer **8**, which adsorbs its first few molecules of hydrogen at −17 kJ/mol (Figure 4), is the slowest while polymers **10** and **13**, which adsorb at 11−12 kJ/mol have overlapping curves. In single file diffusion, molecules cannot pass each other within a pore. Because of this, they are forced to move like pearls on a string; in a single step, a molecule can only diffuse stepwise to the adjacent adsorption site if it is not occupied. In addition, desorption to the gas phase can take place only at the termini of the pores. Because of these effects, adsorption to pores in which single file diffusion takes place is much slower than adsorption to other types of pores. In addition, single-file diffusion has been shown to result in significantly higher activation energies than ordinary diffusion. [69−71] It appears that networks that adsorb their first few molecules of H_2 with the highest adsorption enthalpies tend to be the slowest; however, this cannot be expected to hold for all materials as some structural properties that constrict transport may affect kinetics without affecting thermodynamics. It should be noted that even the slowest adsorbing materials exhibit kinetics that are acceptable for hydrogen storage.

Typically, the enthalpy of adsorption is calculated by applying the van't Hoff equation to isotherms collected at 77 and 87 K. Our materials adsorb substantial amounts of

(65) Ma, S. Q.; Sun, D. F.; Wang, X. S.; Zhou, H. C. *Angew. Chem., Int. Ed.* **2007**, *46*, 2458.
(66) Humphrey, S. M.; Chang, J. S.; Jhung, S. H.; Yoon, J. W.; Wood, P. T. *Angew. Chem., Int. Ed.* **2007**, *46*, 272.
(67) Dybtsev, D. N.; Chun, H.; Yoon, S. H.; Kim, D.; Kim, K. *J. Am. Chem. Soc.* **2004**, *126*, 32.
(68) Jeon, Y. M.; Armatas, G. S.; Heo, J.; Kanatzidis, M. G.; Mirkin, C. A. *Adv. Mater.* **2008**, *20*, 2105.
(69) Liu, H.; Lei, G. D.; Sachtler, W. M. H. *Appl. Catal., A* **1996**, *137*, 167.
(70) Rodenbeck, C.; Karger, J.; Hahn, K. *J. Catal.* **1995**, *157*, 656.
(71) Lei, G. D.; Carvill, B. T.; Sachtler, W. M. H. *Appl. Catal., A* **1996**, *142*, 347.

hydrogen at very low pressures. The cryogenic technique cannot be used to determine the enthalpy of adsorption of the first few molecules of hydrogen because of errors introduced by thermal transpiration at these low pressures. Also, the enthalpy of adsorption is a weak function of temperature. Thus, we calculate adsorption enthalpies from isotherms measured at 298 and 273 K. The initial enthalpy of hydrogen adsorption for polymer **10** is −14 kJ/mol. Polymer **9**, *p*-diaminobenzene hypercrosslinked with tribromobenzene, features a ΔH of hydrogen adsorption as high as −18 kJ/mol. This is the first organic nanoporous material that exhibits an enthalpy of adsorption in the −15 to −20 kJ/mol range, which is highly desired for hydrogen storage at room temperature.[37]

It is interesting to note that within the low-coverage regime, the enthalpy of adsorption increases with the amount of stored hydrogen for many of our polymers. Since these networks contain only very rigid bonds, it seems unlikely that they can swell with the gas. It has been demonstrated previously that materials in which single file diffusion takes place can have significantly higher adsorption enthalpies than materials in which ordinary transport takes place.[71] To explain the positive slopes of plots of enthalpy of adsorption, we must consider the available mechanisms of hydrogen adsorption. For the majority of large surface area hydrogen storage materials, hydrogen is transported in the gas phase via a combination of Fickian, Knudsen, and surface diffusion depending on the pressure of the gas and pore size. Each molecule adsorbed at the surface is free to desorb and re-enter the gas phase upon receiving the Arrhenius energy required to do so. For single-file diffusion pores, the situation is different. Once a particle has entered a pore, it can exit only by waiting for all of the other particles between it and the pore entrance to diffuse out. Within a certain coverage regime, as coverage increases, adsorbed particles become more confined and it becomes more difficult for a particular particle to reach the pore exit. It has been demonstrated previously that properties that typically decrease with coverage such as self-diffusion constants can instead increase with single-file diffusion.[72] It is possible that the regime of increasing adsorption enthalpy seen with the most tightly crosslinked polymers might be due to the predominance of single-file diffusion.

The slope of the plot of enthalpy of adsorption (Figure 4) correlates well with the type crosslinker used in the preparation. For example, the plot for polymer **8**, a polymer that is cross-linked with diiodomethane, has a negative slope, whereas polymer **9**, cross-linked with tribromobenzene, exhibits a positive slope. we suggest that crosslinking with this trivalent moiety affords a tighter network with a larger number of constricted pores and might lead to a higher incidence of single-file diffusion.

Other materials that contain small pores display enhanced enthalpies of adsorption. Jhung, et al. used materials with crystallographically defined pore sizes to demonstrate that the enthalpy of hydrogen adsorption on nanoporous aluminophosphates increases by a factor of 2.5 when the pore size decreases from 1.27 nm × 1.27 nm (1.61 nm^2) to 0.49 nm × 3.0 nm (1.47 nm^2).[40] Similar effects have been demonstrated for porous carbons[73] and Hoffman clathrate derivatives.[74] Recently, microporous poly(aryleneethylene) networks were synthesized in which polymers with small distances between aromatic rings exhibit enthalpies of adsorption as large as −10 kJ/mol and adsorption enthalpies which do not change monotonically with coverage.[12] In addition, theoretical calculations have predicted increasing enthalpy of hydrogen adsorption as pore size decreases.[39] In porous materials such as these, hydrogen interacts with the surface of pore walls via physisorption. In large pores, hydrogen can only interact with one wall at a time. In contrast, a molecule adsorbing in smaller pores can interact with multiple pore walls simultaneously, thus increasing the overall energy of interaction.[41]

In addition to pore size, which is generally a very important characteristic of nanoporous polymers, chemical structure also plays an important role providing for high affinity to hydrogen. The presence of electron-donating substituents on the aromatic rings increases the strength of the hydrogen−polymer interactions and enables adsorption.[75] In contrast, the presence of electron withdrawing groups drastically decreases hydrogen adsorption.[22] Our materials feature numerous aromatic rings that are the primary adsorption sites,[21,28,76,77] these are linked through electron donating the tertiary amine functionalities. We suggest that it is the combination of both favorable chemistry and small pore size that results in the high adsorption enthalpies observed with these polymers.

A palladium-containing catalyst is used in the synthesis of our porous polymers. Because palladium-containing porous materials have been tested for hydrogen storage based on the spillover mechanism,[78−80] we have to consider the possibility that the observed high enthalpies of adsorption could be due to spillover. However, an analysis of the mechanism of this process suggests that spillover is not expected in systems where physisorption of H_2 blocks transport of spillover H. In addition, spillover does not explain the high adsorption ability measured at low pressures and cryogenic temperatures. To verify that the high hydrogen adsorption enthalpies measured are not due to spillover, 1,4-diaminobenzene was crosslinked with tribromobenzene using the Ullman process.[46,48] Although Buchwald syntheses used for much of this work are more effective than Ullman syntheses, the latter do not involve palladium. Using the latter, we may expect less effective crosslinking, fewer pores suitable for single-file adsorption, and adsorption enthalpies

(72) Brandani, S.; Xu, Z.; Ruthven, D. *Microporous Mater.* **1996**, *7*, 323.
(73) Yushin, G.; Dash, R.; Jagiello, J.; Fischer, J. E.; Gogotsi, Y. *Adv. Funct. Mater.* **2006**, *16*, 2288.
(74) Culp, J. T.; Natesakhawat, S.; Smith, M. R.; Bittner, E.; Matranga, C.; Bockrath, B. *J. Phys. Chem.C* **2008**, *112*, 7079.
(75) Lochan, R. C.; Head-Gordon, M. *Phys. Chem. Chem. Phys.* **2006**, *8*, 1357.
(76) Buda, C.; Dunietz, B. D. *J. Phys. Chem.B* **2006**, *110*, 10479.
(77) Spoto, G.; Vitillo, J. G.; Cocina, D.; Damin, A.; Bonino, F.; Zecchina, A. *Phys. Chem. Chem. Phys.* **2007**, *9*, 4992.
(78) Back, C. K.; Sandi, G.; Prakash, J.; Hranisavljevic, J. *J. Phys. Chem. B* **2006**, *110*, 16225.
(79) Rather, S.; Zacharia, R.; Hwang, S. W.; Naik, M.; Nahm, K. S. *Chem. Phys. Lett.* **2007**, *441*, 261.
(80) Anson, A.; Lafuente, E.; Urriolabeitia, E.; Navarro, R.; Benito, A. M.; Maser, W. K. *J. Phys. Chem. B* **2006**, *110*, 6643.

that are lower and should not tend to increase with coverage. The resulting synthesis produced a material with BET and Langmuir surface areas of 66 and 302 m^2/g respectively, and 0.10 cm^3/g of size-selective pores. Figure 4 shows that the enthalpy of hydrogen adsorption to this palladium-free polymer is in the 11−12 kJ/mol range, similar to that of polymer **10**, which was cross-linked using the Buchwald process. The slightly lower adsorption enthalpy and decreasing slope of the adsorption enthalpy plot are likely due to the incomplete network that is obtained via the Ullman reaction.

Conclusions

This study demonstrates that hypercrosslinked networks of aromatic rings with pores that are too small to allow penetration of nitrogen but large enough for hydrogen adsorption can be generated. Their formation takes place when aromatic rings are crosslinked with a trivalent and totally rigid linking group. These lightweight materials exhibit high enthalpies of adsorption for hydrogen reaching up to −18 kJ/mol. This value places them in range that could achieve reversible hydrogen storage at room temperature. However, further development is necessary in order to significantly increase both their surface area and pore volume as our preliminary experiments indicate that polymer **9** stores 0.22 wt % excess H_2 at 273 K and 9 MPa. To produce polymers meeting both thermodynamic and capacity requirements, fast crosslinking reactions must be used. Because the need for a catalyst required in reactions employed in this work imposes mass transfer limitations on kinetics and the catalyst has to be removed from very small pores after the reaction is completed, attention should now focus on noncatalytic approaches to such hypercrosslinked materials.

Acknowledgment. Financial support of this work, including characterization work done at the Molecular Foundry, was provided by the Director, Office of Science, Office of Basic Energy Sciences, Division of Materials Sciences and Engineering, of the U.S. Department of Energy under Contract DE-AC02-05CH11231.

CM802157R